Journal of Applied Mechanics and Technical Physics, Vol. 37, No. 5, 1996

STOCHASTIC FLUTTER OF A ROW OF PLATES IN A TURBULENT BOUNDARY LAYER OF INCOMPRESSIBLE FLOW

V. P. Reutov and G. V. Rybushkina UDC 537.86.187;530.182;533.6.013.42

The nonlinear dynamics of a long row of rectangular plates in a turbulent boundary layer of incompressible fluid is studied in the present paper. The row is aligned with the flow, and the plate edges are immediately adjacent to each other and are not mechanically connected. The analysis is based on the results of [1–3], where the response of the mean flow in a turbulent boundary layer to the flexure of an individual plate and a pair of adjacent plates was determined.

The equations of motion of the row are derived under the same assumptions that were used in [3] to study nonlinear flutter of a pair of adjacent plates (the deflection nonlinearity at a "linear" flow response is taken into account). The case of high-density fluid flow around the row (the apparent additional mass is comparable with the mass of the plates or exceeds it) is considered, which allows us to restrict ourselves to a one-mode plate flexure approximation.

Dowell [4] studied the occurrence of random self-oscillatory regime for supersonic flow around an individual panel. Vol'mir [5] considered periodic self-excited oscillations of a row of plates in supersonic potential flow. No self-excited oscillations arise in strictly potential incompressible (essentially subsonic) flow around the plates [3]. However, these oscillations can occur due to irreversible energy transfer to the plates from the mean flow under the boundary layer that always appears near the exposed surface under real conditions. The case of a turbulent boundary layer is of considerable practical interest. Reutov [3] showed that such a generation mechanism can cause the transition from periodic to chaotic self-excited oscillations (a stochastic flutter) in a system of two adjacent plates. The goal of this paper is to study the features of the onset of dynamic chaos in a long row of plates simulating a large panel surface.

1. Approximation of Close-Range Interaction of Plates in a Long Row. Let us consider a row of identical rectangular plates located at the same level with a rigid surface $y = 0$. The plate dimensions along and across the row are denoted as L_1 and L_2, respectively. The adjacent edges of the plates are fixed with a hinge. The plates are assumed to have a high transverse rigidity, and only their buckling along the row is possible. On the side $y > 0$ the row is exposed to a turbulent boundary layer of incompressible flow in the longitudinal x direction, and, in the half-space $y < 0$, there is an immobile medium with negligibly small density. The boundary-layer thickness δ is constant along the entire row.

We shall confine ourselves to the study of row oscillations in a close-range approximation in which only the relation between adjacent plates in the flow is taken into account. To solve this problem, one can use the equations of one-mode oscillations of a pair of adjacent plates adopted in [3]. Preserving the dimensionless variables adopted in [3], we write the equations of row motion in Lagrangian form (see, for instance, [6]):

$$\frac{d}{dt}\left(\frac{\partial L}{\partial \dot{A}_k}\right) - \frac{\partial L}{\partial A_k} = Q_k. \tag{1.1}$$

Here A_k is the amplitude of the first Galerkin mode of the kth plate flexure (normalized to the plate thickness h), L is the Lagrangian of the system, and Q_k are the generalized nonconservative forces. The Lagrangian of a

Institute of Applied Physics, Russian Academy of Sciences, Nizhnii Novgorod 603600. Translated from Prikladnaya Mekhanika i Tekhnicheskaya Fizika, Vol. 37, No. 5, pp. 52–62, September–October, 1996. Original article submitted March 21, 1995l; revision submitted July 27, 1995.

 0021-8944/96/3705-0658 $15.00

row with a close-range interaction of plates has the form (summation is performed over the all plate numbers)

$$L = \sum_j \Big[\frac{1}{2} M_0 \dot{A}_j^2 + M_1 \dot{A}_j \dot{A}_{j-1} + M_2 \dot{A}_j \dot{A}_{j-2} - \frac{1}{2} B_1 (A_j \dot{A}_{j-1} - \dot{A}_j A_{j-1}) + \frac{1}{2} D_0 A_j^2 + D_1 A_j A_{j-1} - \frac{3}{4} æ A_j^4\Big], \qquad (1.2)$$

where the coefficients M_0, M_1, B_1, D_0, and D_1 are expressed in terms of the parameters defined in [3]: $M_0 = m_0 \equiv \alpha + \alpha_1 a_0$, $M_1 = \alpha_1 a_1$, $B_1 = \alpha_1 V b_1$, $D_0 = d_s \equiv \alpha_1 d_0 V^2 - 1$, $D_1 = \alpha_1 V^2 d_1$; and $æ > 0$. Thus, $\alpha = \gamma/(\gamma + \gamma_0)$, where γ and γ_0 are the plate mass per unit area and the reference additional mass of the fluid, respectively, and $\alpha_1 = 1 - \alpha$. Then the heavy flow ($\gamma/\gamma_0 < 1$) around the row is considered, and all computations, as in [3], are performed for $\alpha = 0.2$. The dimensionless flow velocity is $V = u_\infty k_0/\omega_0$, where u_∞ is the free-stream velocity outside the boundary layer, $k_0 = \pi/L_1$ is the flexural wavenumber, and ω_0 is the characteristic frequency of plate oscillations with allowance for the apparent additional mass of the fluid [the time in (1.1) and (1.2) is also normalized to ω_0)]. The coefficients a_0, a_1, b_1, d_0, and d_1 which are weakly dependent on the Reynolds number are calculated in [2, 3][1] for $k_0\delta = 1$. The theory was developed for a quasi-two-dimensional flexure of the plates ($L_2 \gg L_1$), and numerical values were found for $L_2/L_1 = 3$.

The nonconservative forces Q_k take into account the plate-material losses and the frequency-dependent energy transfer between the oscillating surface and the mean boundary-layer flow:

$$Q_k = -2\bar{r}\dot{A}_k - \alpha_1\beta(V^2\xi_k + V g_0 \dot{A}_k) + \alpha_1\beta_1 V^2 \eta_{k-1},$$
$$\ddot{\xi}_k + \sigma_0 V \dot{\xi}_k + V^2 c_0^2 \xi_k = q_0 V \dot{A}_k - s_0 V^2 A_k, \quad \ddot{\eta}_k + \sigma_1 V \dot{\eta}_k + V^2 c_1^2 \eta_k = q_1 V \dot{A}_k - s_1 V^2 A_k. \qquad (1.3)$$

The values of the coefficients g_0, β, β_1, $\sigma_{0,1}$, $c_{0,1}$, and $q_{0,1}$ are given in [3], and ξ_k and η_k are auxiliary variables that describe the contribution to Q_k of the plate numbered k and the upstream plate adjacent to it. The normalized loss coefficient $\bar{r}$ can be expressed in terms of the quality factor Q_f of the natural oscillations of the plate in vacuum [1]: $\bar{r} = (1/2Q_f)\sqrt{\alpha}$. Note that the nonconservative forces make a little contribution to (1.1) since β, β_1, and $\bar{r} \ll 1$. The coefficient M_0 in (1.2) characterizes the mass of each plate with the additional mass of the fluid, and M_1 describes the interaction of neighboring plates via acceleration of their surfaces (mutual-additional-mass type effects). The coefficient M_2 taking into account the coupling via acceleration between plates with numbers that differ by two will be defined below. Let us note that the coefficient B_1 characterizes the "inertial-drift" coupling between the plates (which is due to the motion of their surfaces and the presence of flow over it), and the coefficients D_0 and D_1 are responsible for the intrinsic and mutual elasticity of the plates in the flow. In the absence of Q_k, Lagrangian (1.2) describes the "quasipotential" flow around the plates [1–3].

System (1.1)–(1.3) is readily generalized for a row of plates located on a distributed springy base with elasticity coefficient K_E per unit area. (An elastic surface model with a springy base is considered in [7].) For this, one should define ω_0 and $æ$ as $\omega_0 = [(Dk_0^4 - Nk_0^2 + K_E)/\gamma_0]^{1/2}$ and $æ = 1/(1 - N/k_0^2 D + K_E/k_0^4 D)$ (see the notation in [3]). In addition, the same system will describe a symmetric two-side flow around a row of plates if we make the formal substitution $\alpha_1 \to 2\alpha_1$ in (1.1)–(1.3) preserving the definitions of α and α_1.

2. Transition to the Hamiltonian Description and Substantiation of Approximation of Close-Range Interaction. As is seen from (1.1)–(1.3), when the plates are coupled via acceleration ($M_{1,2} \neq 0$), the second derivatives $\ddot{A}_k$ are not expressed explicitly in terms of $\dot{A}_k$ and A_k, and this makes it impossible to write the system as the first-order equations. Explicit expressions for $\ddot{A}_k$ are found by solving a linear system of algebraic equations whose order equals the number of plates in the row and contain velocities $\dot{A}_k$ and flexures A_k of all plates. It is clear, however, that with decreasing contributions of higher coupling via acceleration, there is no need to take into account the effect of flexure of all plates on $\ddot{A}_k$. A sequential realization of approximation of the close-range interaction for coupling via acceleration is possible if we pass to the Hamiltonian description of row motion.

---

[1]The coefficients b_1 and d_1 are misprinted in [3]. Their true values are $b_1 = -0.43$ and $d_1 = -0.10$.

Let us introduce the Hamiltonian H and generalized momenta p_k using the known formulas [6]

$$H = \sum_j \dot{A}_j \frac{\partial L}{\partial \dot{A}_j} - L, \quad p_k = \frac{\partial L}{\partial \dot{A}_k}. \tag{2.1}$$

Here the subscripts j and k run through the numbers of all plates. The substitution of (1.2) into the second relation of (2.1) yields

$$p_k = M_0 \dot{A}_k + M_1(\dot{A}_{k+1} + \dot{A}_{k-1}) + M_2(\dot{A}_{k+2} + \dot{A}_{k-2}) - \frac{1}{2} B_1(A_{k+1} - A_{k-1}). \tag{2.2}$$

We shall seek an explicit expression for the flexural velocities $\dot{A}_k$ in terms of p_k in the form of a series of perturbation theory in coupling between the plates. Restricting the discussion to zeroth- and first-order terms, we have

$$\dot{A}_k = \frac{1}{M_0}\left[p_k - \frac{M_1}{M_0}(p_{k+1} + p_{k-1}) - \frac{M_2}{M_0}(p_{k+2} + p_{k-2}) + \frac{1}{2} B_1(A_{k+1} - A_{k-1})\right]. \tag{2.3}$$

Substituting (2.3) into (1.2) and (2.1) and ignoring second-order terms with respect to coupling, we obtain a Hamiltonian for the row in the approximation of close-range interaction:

$$H = \sum_j \left[\frac{1}{2M_0} p_j^2 - \frac{M_1}{M_0^2} p_{j-1}p_j - \frac{M_2}{M_0^2} p_{j-2}p_j \right.$$
$$\left. + \frac{B_1}{2M_0}(p_{j-1}A_j - p_jA_{j-1}) - \frac{1}{2} D_0 A_j^2 - D_1 A_{j-1}A_j + \frac{3}{4} æ A_j^4\right]. \tag{2.4}$$

The canonical equations generated by Hamiltonian (2.4) include system (2.3) and momentum equations

$$\dot{p}_k = D_0 A_k + D_1(A_{k+1} + A_{k-1}) + \frac{B_1}{2M_0}(p_{k+1} - p_{k-1}) - 3æ A_k^3 + Q_k. \tag{2.5}$$

The full system of equations for row motion (2.3), (2.5), and (1.3) is convenient for computer solution, since it is easily reduced to a system of first-order equations. For a row of finite length one should equate to zero the variables A_k and p_k with subscript values beyond the scope of plate numbers.

Let us consider the stability of the zeroth stationary flexure of an infinite row against wave perturbations of the form

$$A_n = \frac{1}{2} A e^{in\vartheta - i\omega t} + \text{complex conjugate}, \tag{2.6}$$

where A is the complex amplitude of the wave; ω is its frequency, and ϑ is the phase shift per one coupling (the wavenumber of a running wave). For a conservative model ($Q_k \to 0$) we obtain a dispersion equation from the linearized system (2.3) and (2.5):

$$M\left(\omega + \frac{B_1}{M_0} \sin\vartheta\right)^2 + D_s = 0, \tag{2.7}$$

where $M = M_0^2/(M_0 - 2M_1 \cos\vartheta - 2M_2 \cos 2\vartheta)$ and $D_s = D_0 + 2D_1 \cos\vartheta$. Its solutions have the form

$$\omega_{1,2} = -\frac{B_1}{M_0} \sin\vartheta \pm \sqrt{-\frac{D_s}{M}}. \tag{2.8}$$

Taking into account the dependence of D_s and M on V, it is easy to show that for $V > V_c = 1/\sqrt{\alpha_1 d_0 + 2\alpha_1 d_1 \cos\vartheta}$ the roots are complex-conjugate ("reactive" instability of the flexure arises). The quasi-static instability (divergence) of disturbances with a counter-phase flexure of adjacent plates $\vartheta = \pi$ has minimum critical velocity V_c. For the numerical values of the coefficients given in [3] $V_c \simeq 1.38$.

To clarify the role of distant coupling between the plates, we studied row oscillations in uniform potential flow. We confine ourselves to a brief description of the results of this analysis. In a comparatively simple potential flow model, it is possible to derive a full system of equations of motion of the row taking into account both an infinite set of Galerkin flexural modes and the entire set of relations between the modes on different plates. Restricting ourselves to a finite number of modes, we easily obtain a dispersion equation for small oscillations (2.6) as a polynomial in ω (whose power is equal to the doubled number of modes). The coefficients of this equation are infinite sums over the length of coupling j between the plates ($j = 0, 1, 2 \ldots$). The dependence of the components of these sums on j is found explicitly, and this enables one to solve the question about their convergence.

In the one-mode plate flexure model, summation over "inertial-drift" and elastic higher-order couplings yields a finite result for any ϑ, couplings with numbers $j \geqslant 2$ making a minor contribution to the sums. At the same time, summation of contributions of distant couplings via acceleration leads to a logarithmic singularity for $\vartheta = 0$, which corresponds to an infinite additional mass (calculated for one plate) for synchronous oscillations of all plates of an infinite row. This divergence of additional mass is similar to that discussed in [2] for a two-dimensional flexure of a single infinite plate.

The calculations showed that an increase in the number of summed couplings via acceleration leads to a sharp increase in the sum within a comparatively narrow range of values of $|\vartheta|$ near $\vartheta = 0$. Outside this region, only the close-range interaction between the plates can be taken into account with an acceptable accuracy. Analyzing the expression for M in (2.7), one can easily see that the effect of increasing additional mass for flexures with $\vartheta \to 0$ can be taken into account phenomenologically within the framework of approximate system (2.3) and (2.5). Precisely for this purpose the coupling via acceleration was derived in (1.1) for plates whose numbers differ by two (the term $\sim M_2$). The effect of a sharp increase in additional mass for small ϑ (with a comparatively small variation of M in the main region of values of ϑ) is achieved if M_2 is chosen from the condition $M|_{\vartheta=0} \gg M_0$. This correction is necessary if substantial synchronous plate flexures arise in the approximation of the close-range interaction for some reasons. Since the growth of additional mass for $\vartheta \to 0$ leads to suppression of synchronous plate oscillations, it is natural to assume that the dynamics of the row depends more greatly on the fact of suppression itself than on the way of its realization. In the calculations below the coefficient M_2 is determined from the condition $M_0 - 2M_1 - 2M_2 = 0.2M_0$.

Within the framework of the full system of equations we also considered two-mode plate oscillations with a variable-sign periodic flexure in an infinite row ($\vartheta = \pi$). Calculations of heavy fluid flow showed that for $V \leqslant 1.5V_c$ allowance for the second mode has a minor effect on the behavior of the roots of (2.8). Only with a further increase in V is the deviation from (2.8) observed, and the frequency of natural oscillations due to the second mode decreases. The correctness of approximation of the close-range interaction for a dissipative coupling was supported in [2, formulas (5.3) and (5.4)].

Thus, the approximation of close-range interaction for one-mode oscillations of an infinite row of plates supplemented by the phenomenological consideration of the effect of increasing additional mass in synchronous flexure of the plates can be used to describe an actual row at flow velocities that are not too high compared with the critical divergence velocity.

3. The Ginzburg–Landau Equation for Wave Disturbances Near the Stability Threshold. The allowance in (2.5) for non-conservative forces of the flow response to the row flexure leads to resistive instability which was studied in [1] for a variable-sign flexure ($\vartheta = \pi$). It is subcritical with respect to divergence, since it has a critical velocity $V_c' < V_c$.

To investigate this instability for an arbitrary ϑ, let us define the dissipative portion of the flow response to the surface flexure (2.6) as $Y(\omega, \vartheta) = \hat{Q}/A$ [$\hat{Q}$ is the complex amplitude of the harmonic $\exp(in\vartheta - i\omega t)$ of the Q_n distribution]. Using (1.3), one can write an expression for Y as

$$Y = 2i\bar{r}\omega - \alpha_1 \beta V^2 \Big[\varphi\Big(\frac{\omega}{V}\Big) - ig_0 \frac{\omega}{V}\Big] + \alpha_1 \beta_1 V^2 \varphi_1 \Big(\frac{\omega}{V}\Big) e^{-i\vartheta}, \tag{3.1}$$

where φ and φ_1 are the rational functions defined by relations (1.3) and (1.5) from [3].

The dispersion equation for the linear problem is obtained from (2.8) after the formal substitution $D_s \to D_s + Y(\omega, \vartheta)$. Solving it by the method of perturbations with respect to small Y, we obtain the resistive instability increment in the subcritical region ($V < V_c$):

$$\Gamma = \operatorname{Im} \omega = -\frac{\operatorname{Im} Y}{2M(\omega + (B_1/M_0) \sin \vartheta)} \bigg|_{\omega = \Omega(\vartheta)}. \tag{3.2}$$

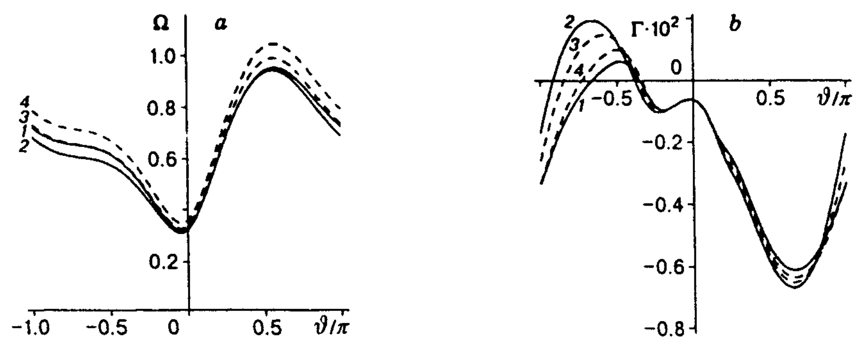

Fig. 1

Here, $\Omega(\vartheta) = \mathrm{Re}\,\omega_1 > 0$ is the wave frequency in the conservative system [see (2.8)]. The critical velocity of resistive instability V_c' depends on $\bar{r}$. For the value $\bar{r} = 0.004$ which is used in all further calculations, instability arises for $V_c' = 0.73$, $\vartheta_c \simeq -0.36\pi$, and $\omega_c \simeq 0.60$.

Figure 1 shows the dispersion characteristics of the row (a) and the resistive instability increment (b) constructed using (3.1) and (3.2) (curves 1 and 2 correspond to $V = 0.77$ and 0.8). Note that instability first arises for $\vartheta \neq \pm\pi$, and the phase velocity of disturbances at the threshold of stability loss is directed upstream. At first glance, the latter fact contradicts the well-known results of the theory of wave stability on elastic coatings when streamwise disturbances increase [7]. It should be taken into account, however, that disturbance (2.6) corresponds to a wide three-dimensional spectrum of the surface flexure with respect to the x coordinate including both "forward" and "backward" waves. Because of the fairly large relative elasticity for adjacent plates (see [3]), the direction of the energy exchange with the flow depends not only on their oscillation frequency ω but also on the phase shift ϑ. The wave dispersion in a conservative system in this case induces a phase ratio of the flexures such that the instability threshold is exceeded for the first time for the upstream waves.

If the critical velocity V_c' is slightly exceeded, a narrow wave spectrum for ϑ is excited (curve 1 in Fig. 1). In this case, one can derive the Ginzburg–Landau equation for weakly nonlinear modulated waves, which is now one of the basic models used to study the dynamic chaos [8, 9].

The dispersion equation for weakly nonlinear waves is obtained from (2.7) after substituting $D_s \to D_s - (9/4)æ|A|^2$. Accordingly, with accuracy up to the second-order amplitude corrections, the wave frequency takes the form

$$\Omega = \tilde{\Omega}(|A|^2, \vartheta) \equiv \Omega(\vartheta) + \rho|A|^2 \quad \left(\rho = \frac{9æ}{8\big(\Omega + (B_1/M_0)\sin\vartheta\big)}\right). \tag{3.3}$$

When calculating the increment Γ in (3.2) one should use the frequency with nonlinear correction (3.3). Considering the expression for Γ as a function of ω before substituting $\omega = \tilde{\Omega}$ into it, let us use its passage through zero for $\omega = \omega_*(\vartheta)$. [For $\omega = \omega_*$ the loss is compensated by the energy supply from the flow. Obviously, $\omega_c = \omega_*(\vartheta_c)$.] Using a linear approximation of this function, we can write $\Gamma \approx \mu[\omega - \omega_*(\vartheta)]$, where $\mu(\vartheta) = \partial\Gamma/\partial\omega\big|_{\omega=\omega_*} < 0$. As a result we obtain an expression for the complex frequency of nonlinear waves with accuracy up to second-order amplitude corrections:

$$\tilde{\Omega} = \Omega(\vartheta) + \rho(\vartheta)|A|^2 + i\Gamma(\vartheta) + i\mu(\vartheta)\rho(\vartheta)|A|^2. \tag{3.4}$$

The main part of the solution of a weakly nonlinear problem can be presented in the form of (2.6) where $\vartheta = \vartheta_0$ and $\omega = \omega_0$ are the wave parameter values at the maximum of the increment $\Gamma(\vartheta)$ (which are, generally speaking, different from ϑ_c and ω_c), and the complex amplitude A is a slowly changing function of n and t.

Multiplying (3.4) by $A(n,t)\exp(in\vartheta - i\omega t)$ and applying the standard procedure of Fourier transform

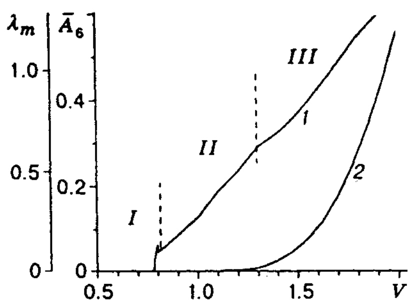

Fig. 2

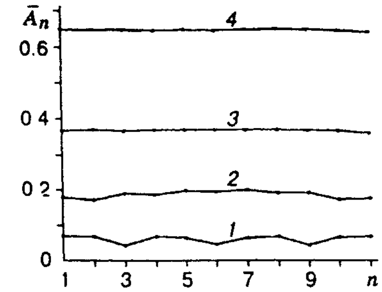

Fig. 3

for narrow wave packets [10], we obtain a one-dimensional Ginzburg–Landau equation in the form

$$\frac{\partial A}{\partial t} + \frac{1}{2}(\Gamma_0'' - i\Omega_0'')\frac{\partial^2 A}{\partial n^2} = \varepsilon A - (i + |\mu_0|)\rho_0|A|^2 A, \tag{3.5}$$

where $\varepsilon = \Gamma(\vartheta_0)$ is the supercriticality of the flow–row system; $\Gamma_0'' < 0$, Ω_0'', μ_0, and ρ_0 are the values of $\partial^2\Gamma/\partial\vartheta^2$, $\partial^2\Omega/\partial\vartheta^2$, μ, and ρ for $\vartheta = \vartheta_0$. Equation (3.5) is written in the frame of reference moving with the wave group velocity (the substitution $t_{\text{new}} = t$, $n_{\text{new}} = n - (\partial\Omega/\partial\vartheta_0)t$ is performed after which the subscript "new" is omitted).

A characteristic feature of the Ginzburg–Landau equation (3.5) is its "quasi-conservative" structure, which is manifested in small values of dissipative terms: $|\mu_0| \ll 1$ and $|\Gamma_0''| \ll |\Omega_0''|$. This small dissipative nonlinearity, however, plays a principal role, since it limits the instability arising at $\varepsilon > 0$. The small term $\sim \Gamma_0''$ should also be preserved in (3.5), since it limits the spectral width of the instability region for ϑ (curve 1 in Fig. 1b near $\vartheta = \vartheta_0 \approx 0.5\pi$).

Equation (3.5) has a solution in the form of a steady-state wave

$$A = \sqrt{\varepsilon/|\mu_0|\rho_0}\exp(-i\varepsilon t/|\mu_0|).$$

The well-known criterion of the occurrence of modulation instability for the normalized Ginzburg–Landau equation [9] written in terms of the coefficients of (3.5) takes the form $\Omega_0'' < -|\Gamma_0''\mu_0|$. This instability has no threshold of supercriticality. In addition, since the dissipative terms are small, the above condition is in fact coincident with the Lighthill condition of the occurrence of modulation instability in the conservative problem in [10], which, for (3.5), takes the form $\Omega_0'' < 0$. As is seen from Fig. 1, this condition is satisfied for weakly supercritical waves. Thus, small dissipation determines the generation level, and the modulation instability remains the same as in a conservative system. It was shown in some papers (see, for example, [11–13]) that the one-dimensional Ginzburg–Landau equation describes various regimes of dynamic chaos.

4. Results of Numerical Investigation of Random Self-Excited Oscillations. System (2.3), (2.5), and (1.3) was solved numerically for a row of 11 plates. The numerical scheme included the fourth-order Runge–Kutta technique and the variable step algorithm with accuracy control. Arbitrary initial distributions of small flexures A_k and zero values of p_k, ξ_k, η_k, $\dot{\xi}_k$, and $\dot{\eta}_k$ were set. In Eqs. (2.5) it was assumed that $æ = 1$, which did not restrict the generality of consideration [3]. Time averaging, which is denoted below by angle brackets, was performed by summation of the values of the averaged quantity at equidistant time moments and subsequent division of the result by the number of points. The standard amplitude of the plates flexure was determined by the formula $\bar{A}_n = \sqrt{\langle (A_n - \langle A_n\rangle)^2\rangle}$.

No self-excited oscillations appear with rather large losses in the plates $\bar{r}$. Ignoring the contribution to Q_k due to the energy exchange with the boundary layer (β, $\beta_1 \to 0$), we obtain the following relation

$$\frac{dH}{dt} = -2\bar{r}\sum_j \dot{A}_j^2 \leqslant 0. \tag{4.1}$$

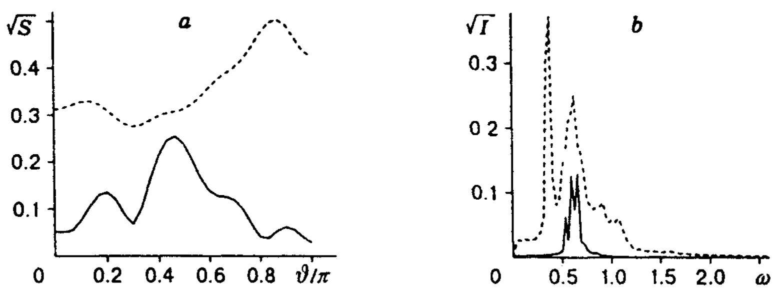

Fig. 4

It follows from (4.1) that the system tends to an equilibrium state that coincides with one of the local minima of the Hamiltonian H. Steady flexures different from zero arise for $V > V_c$. In particular, the steady state of an infinite row is easily found from (2.3) and (2.5) in the form of a variable-sign flexure: $A_n = (-1)^n\sqrt{(D_0 - 2D_1)/3æ}$. Numerical solution of the equations showed that a row with large losses in the plates demonstrates the multistability property (the multiplicity of asymptotic states) typical of dissipative distributed systems [8, 9]. Each of these states is a sequence of segments with a variable-sign flexure. At sites of contact of the segments the flexure of adjacent plates is identical, and this can be regarded as the appearance of defects in a periodic "grid." The appearance of defects can be attributed to the arbitrariness in selecting the reference point ("phase") in a solution with a variable-sign flexure.

The self-excited oscillations in a row with small losses were studied using the numerical integration of Eqs. (2.3), (2.5), and (1.3) for $\bar{r} = 0.004$. The main results are presented in Figs. 2–5. Curve 1 in Fig. 2 is the standard amplitude of the oscillations of the central plate flexure $\bar{A}_6$ versus the flow velocity V, the regions with qualitatively different oscillatory regimes being numbered I–III. It is widely known that one of the basic criteria of existence of a random attractor in the phase space of a system is the presence of positive Liapunov factors [10, 14]. The largest of them, λ_m, determines the "divergence" velocity of phase trajectories on this attractor. Curve 2 in Fig. 2 shows the behavior of the main Liapunov factor λ_m.

Figure 3 shows the $\bar{A}_n$ distribution along the row for various flow velocities (curves 1–4 correspond to $V = 0.8$, 1.1, 1.5, and 2.0). The space and time spectra of the flexure rate $\dot{A}_k$ are presented in Figs. 4 and 5 [the solid curves in Fig. 4 correspond to $V = 0.8$, and the dashed curves to $V = 1.1$; Fig. 5 illustrates the spectra for $V = 1.5$ (solid curves) and $V = 2$ (dashed curves)]. The space power spectrum $S(\vartheta)$ was calculated using the formula $S = \langle|\dot{A}_\vartheta|\rangle/n_t$, where n_t is the number of couplings in the row and $\dot{A}_\vartheta$ is the Fourier transform for the discrete function $\dot{A}_n$. The time power spectra $I(\omega)$ were calculated for the central plate using the procedure described in [3]. Figure 6 shows the space correlation coefficient of the flexure oscillations with respect to the central plate $K = \langle(A_6 - \langle A_6\rangle)(A_n - \langle A_n\rangle)\rangle/\bar{A}_6\bar{A}_n$.

As is seen from Fig. 3, the intensity distribution of oscillations along the row is nearly uniform practically for each flow velocity. This indicates a minor role of the wave transfer of power along the row. Therefore, it seems quite natural that the critical velocity of excitation of oscillations (see Fig. 2) is close to the value V_c' found in Section 3 for a single wave in an infinite row. A regime with a periodic time modulation of oscillations is observed in a very narrow region I in Fig. 2. The carrier frequency of the oscillations fits approximately the linear theory maximum increment (Fig. 1b). This picture is in good agreement with that predicted in Section 3 on the basis of the Ginzburg–Landau equation.

The oscillations generated in region II in Fig. 2 have several typical peaks in space and time spectra. Since the row is not too long, the discrete peaks of the space spectrum are considerably smeared (by the value $\Delta\vartheta \simeq 2\pi/n_t = 0.2$). The transition to the chaotic regime takes place in region II near its boundary with region I. The main Liapunov factor λ_m is very small here, and the place where it changes sign cannot be established accurately because of the calculation uncertainty. The existence of random self-induced oscillations in the major part of region II is supported by the positive λ_m (see Fig. 2).

As is seen from Fig. 4a, there are peaks with the wavenumbers $\vartheta_1/\pi = 0.68$, $\vartheta_2/\pi = 0.47$, and

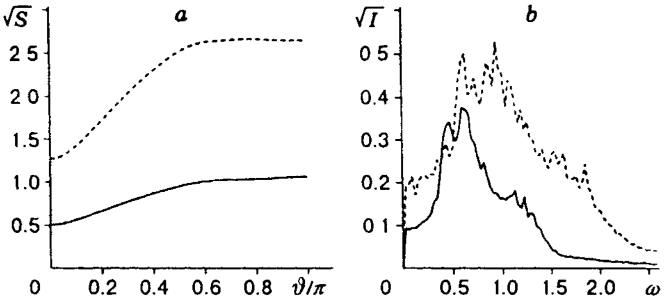

Fig. 5

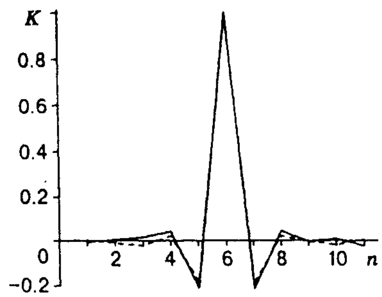

Fig. 6

$\vartheta_3/\pi = 0.9$, and also $\vartheta'/\pi = 0.2$ in the space spectrum for $V = 0.8$. The frequency spectrum peaks have the frequencies $\omega_1 = 0.60$, $\omega_2 = 0.54$, and $\omega_3 = 0.66$. Using the dispersion curve 2 in Fig. 1a, one can easily see that the pairs of values (ω_1, ϑ_1), (ω_2, ϑ_2), and (ω_3, ϑ_3) correspond approximately to the upstream waves of the linear problem. The peak $\vartheta'/\pi = 0.2$ can be explained by the presence of reflected waves in the row that have close frequencies $\omega_{1,2,3}$ (see the dispersion branch 2 at $\vartheta > 0$). The wave (ω_1, ϑ_1) is at the increment maximum of the linear problem (Fig. 1b). The occurrence of waves (ω_2, ϑ_2) and (ω_3, ϑ_3) can be explained by the fact that a four-wave resonance interaction arises in the row: $2\omega_1 \approx \omega_2 + \omega_3$ and $2\vartheta_1 \approx \vartheta_2 + \vartheta_3$. This process can be regarded as the result of transformation of the modulation instability described by the Ginzburg–Landau equation since the waves-satellites move away from the fundamental wave with an increase in V due to the rapid expansion of the instability region for ϑ.

The ratio of intensities of the generated waves is strongly affected by their nonresonance (energetic) interaction. The conservative cubic nonlinearity leads to a nonlinear shift of the wave frequency, owing to which the dependence of the increment on frequency is transformed into its dependence on amplitude. To illustrate this property, let us find the increment of a weak perturbation with wavenumber ϑ_α and frequency $\omega_\alpha = \Omega(\vartheta_\alpha)$ in the presence of a strong disturbance with wavenumber $\vartheta \neq \vartheta_\alpha$ and amplitude A. The dispersion equation for such a "sample" disturbance is obtained by substituting $D_s \to D_s - (9/2)æ|A|^2, \vartheta \to \vartheta_\alpha$ in (2.8). Curves 3 and 4 in Fig. 1 show the behavior of the test wave increment for $\bar{A}_6 = |A|/\sqrt{2} = 0.1$ and 0.15. It follows from the presented dependence, in particular, that an intense disturbance (ω_2, ϑ_2) shifts the increment maximum toward smaller values of $|\vartheta|$ to attenuate the growth of the wave (ω_1, ϑ_1), which is at the increment maximum of the linear problem. Thus, one can assume that dynamic chaos in region II results from resonance and energetic interaction of several quasi-harmonic waves.

A "developed" chaos regime characterized by continuous space and time spectra (see Fig. 5) is observed in region III in Fig. 2. The space spectra in region III have no explicit peaks, and their maximum is at π-oscillations. The concentration of the energy of space harmonics at π-oscillations is associated with the growing tendency of adjacent plates to counter-phase flexure at high velocities, which is due to the potential flow streamlines curvature [3]. The counter-phase character of flexure and rapid loss of correlation of random oscillations along the row are illustrated by the space correlation function shown in Fig. 6.

The boundary between regions II and III is rather conventional and corresponds approximately to the critical divergence velocity V_c (see Section 1). The development of strong stochasticity in region III characterized by high values of λ_m can be explained by the occurrence of separatrix contours in the phase portrait of individual oscillators plates. The chaos results from the "phase mixing" under the action of conservative couplings between the plates just as it takes place in the case of two hinged plates [3]. The frequency spectra in Fig. 5 are also similar to those obtained in [3].

Calculations show that the additional-mass correction for small $|\vartheta|$ discussed in Section 2 affects the oscillation parameters only in regions I and II in which, in the absence of correction, peaks can occur in the space spectrum for small $|\vartheta|$. This is not significant for a "developed" chaos, since the spectrum is shifted toward π-oscillations even under the action of close couplings.

Thus, a model of close interaction of plates in a long row exposed to a turbulent boundary layer is suggested in the present paper. Random regimes of self-induced oscillations of a long row are studied on the basis of this model. All the calculations are performed for "heavy" incompressible flow around a row of plates. It is shown that the features of self-induced oscillations in the "subcritical" region (with respect to the flexure divergence) can be explained in terms of waves. A principal difference of self-induced oscillations in a long row from those in a system of two hinged plates is that stochasticity appears in a long row nearly immediately after the occurrence of instability. In addition, the higher values of the main Liapunov factor and a more rapid loss of "memory" of the random motion about the external effects are typical of a long row.

This work was supported by the Russian Foundation for Fundamental Research (Grant No. 93-05-8075) and International Science Foundation (Grant No. NOV000).

REFERENCES

1. V. P. Reutov, "Instability of the periodic flexure of a panel surface in a turbulent boundary layer," *Prikl. Mech. Tekh. Fiz.*, No. 4, 74–83 (1992).
2. V. P. Reutov, "Instability of flexural vibrations of plates in a turbulent boundary layer," *Prikl. Mech. Tekh. Fiz.*, No. 1, 108–115 (1993).
3. V. P. Reutov, "Nonlinear flutter of plates in the turbulent boundary layer of a weakly compressible flow," *Prikl. Mekh. Tekh. Fiz.*, No. 2, 58–66 (1993).
4. E. N. Dowell, "Flutter of a buckled plate as an example of chaotic motion of a deterministic autonomous system," *J. Sound Vib.*, **85**, No. 3, 333–344 (1982).
5. A. S. Vol'mir, *Nonlinear Dynamics of Plates and Shells* [in Russian], Nauka, Moscow (1972).
6. Paul Appell, *Theoretical Mechanics* [Russian translation], Fizmatgiz, Moscow (1960), Vol. 2.
7. P. W. Carpenter and A. D. Garrad, "The hydrodynamic stability of flow over Kramer-type compliant surfaces. Part 2: Flow induced surface instabilities," *J. Fluid Mech.*, **170**, 199–231 (1986).
8. M. I. Rabinovich and M. M. Sushchik, "Regular and chaotic dynamics of structures in fluid flows," *Usp. Fiz. Nauk*, **160**, No. 1, 1–64 (1990).
9. M. I. Rabinovich, A. L. Fabrikant, and L. Sh. Tsimring, "Finite-difference space disorder," *Usp. Fiz. Nauk*, **162**, No. 8, 1–42 (1992).
10. M. I. Rabinovich and D. I. Trubetskov, *Introduction to Oscillation and Wave Theory* [in Russian], Nauka, Moscow (1984).
11. Y. Kuramoto, *Chemical Oscillations, Waves and Turbulence*, Springer-Verlag, Berlin (1984).
12. M. V. Bazhenov, M. I. Rabinovich, and A. L. Fabrikant, "The amplitude-phase turbulence transition in the Ginzburg–Landau model as a critical phenomenon," *Phys. Lett. A*, **163**, 87–94 (1992).
13. S. Popp, O. Stiller, I. Aranson, et al., "Localized hole solution and spatiotemporal chaos in the 1D complex Ginzburg–Landau equation," *Phys. Rev. Lett.*, **70**, No. 25, 3380–3383 (1993).
14. H. G. Schuster, *Deterministic Chaos: An Introduction*, Physik-Verlag, Weinheim (1984).